Low-Dimensional Organically Templated Uranium Fluorides $(C_5H_{14}N_2)_2U_2F_{12}\cdot 2H_2O$ and $(C_2H_{10}N_2)U_2F_{10}$: Hydrothermal Syntheses, Structures, and Magnetic Properties

Philip M. Almond,[†] Laura Deakin,[‡] Melissa J. Porter,[†] Arthur Mar,[‡] and Thomas E. Albrecht-Schmitt*,[†]

Departments of Chemistry, Auburn University, Auburn, Alabama 36849, and University of Alberta, Edmonton, Alberta, Canada T6G 2G2

Received May 2, 2000. Revised Manuscript Received June 27, 2000

Two new organically templated U(IV) fluorides, $(C_5H_{14}N_2)_2U_2F_{12}\cdot 2H_2O$ (**AU1-1**) and $(C_2H_{10}N_2)U_2F_{10}$ (**AU2-1**), have been prepared from the reaction of UO_3 with HF and homopiperazine ($C_5H_{12}N_2$) at 200 °C in aqueous media. These compounds have been characterized by single-crystal X-ray diffraction, elemental analysis, and magnetic susceptibility measurements. Crystallographic data: **AU1-1**, monoclinic, space group $P2_1/c$, a = 9.272(4) Å, b = 12.314(4) Å, c = 18.475(7) Å, β = 90.32(3)°, Z = 4; **AU2-1**, monoclinic, space group $C2/c$, a = 16.038(8) Å, b = 7.131(3) Å, c = 8.782(4) Å, β = 91.75(4)°, Z = 4. **AU1-1** consists of face-sharing UF_9 tricapped trigonal prisms that form one-dimensional chains that further hydrogen-bond with diprotonated homopiperazine and water molecules. **AU2-1** forms, in part, from the cleavage of homopiperazine to yield diprotonated ethylenediamine, which serves to template the formation of uranium fluoride layers. These layers consist of edge- and corner-sharing UF_9 tricapped trigonal prisms. The variable-temperature magnetic susceptibility of **AU1-1** is consistent with antiferromagnetic interactions between U(IV) centers, with μ_{eff}(300 K) = 4.37 μ_B/f.u. and θ = −1.3 K. The magnetization of **AU1-1** at 2 K displays an irreversible metamagnetic-like transition at H_c = 3.60 T. The magnetic susceptibility for **AU2-1** (μ_{eff}(300 K) = 4.58 μ_B/f.u.) with θ = +21 K suggests the presence of weak ferromagnetic interactions within the $[U_2F_{10}]^{2-}$ layers.

Introduction

Hydrothermal reaction conditions provide facile access to a wide variety of new solid-state materials.[1,2] These materials are typified by low-dimensional and open-framework structures[3−10] which lend themselves to applications such as molecular sieving and catalysis.[11−16] Under mild conditions (<250 °C), inorganic/organic hybrids can be prepared, where the organic portion templates the inorganic architecture. While the exact role of these structure-directing agents is the subject of considerable debate,[17] the use of organic templates has led to a number of previously unobserved structures.

Recent interest in hydrothermal syntheses has focused heavily on metals with variable coordination preferences such as V,[18−25] Fe,[4,6,9,26−30] and Co,[31−34]

[†] Auburn University.
[‡] University of Alberta.

(1) Rabenau, A. *Angew. Chem., Int. Ed. Engl.* **1985**, *24*, 1026.
(2) Kolis, J. W.; Korzenski, M. B. In *Chemical Synthesis Using Supercritical Fluids*; Jessop, P. G., Leitner, W., Eds.; Wiley-VCH: New York, 1999; pp 213−241.
(3) For a recent review, see: Cheetham, A. K.; Férey, G.; Loiseau, T. *Angew. Chem., Int. Ed. Engl.* **1999**, *38*, 3268 and references therein.
(4) Corbin, D. R.; Whitney, J. F.; Fultz, W. C.; Stucky, G. D.; Eddy, M. M.; Cheetham, A. K. *Inorg. Chem.* **1986**, *25*, 2279.
(5) Riou, D.; Taulelle, F.; Férey, G. *Inorg. Chem.* **1996**, *35*, 6392.
(6) Feng, P.; Bu, X.; Stucky, G. D. *Nature* **1997**, *388*, 735.
(7) Feng, P.; Bu, X.; Stucky, G. D. *Chem. Mater.* **1999**, *11*, 3025.
(8) Li, H.; Eddaoudi, M.; Yaghi, O. M. *Angew. Chem., Int. Ed. Engl.* **1999**, *38*, 653.
(9) Choudhury, A.; Natarajan, S.; Rao, C. N. R. *Chem. Mater.* **1999**, *11*, 2316.
(10) Riou-Cavellec, M.; Sanselme, M.; Férey, G. *J. Mater. Chem.* 2000, *10*, 745−748.
(11) Wilson, S. T.; Lok, B. M.; Messina, C. A.; Cannan, T. R.; Flanigen, E. M. *J. Am. Chem. Soc.* **1982**, *104*, 1146.
(12) Flanigen, E. M.; Patton, R. L.; Wilson, S. T. *Stud. Surf. Sci. Catal.* **1988**, *37*, 13.
(13) Gier, T. E.; Stucky, G. D. *Nature* **1991**, *349*, 508.
(14) Xu, R.; Chen, J.; Feng, C. *Stud. Surf. Sci. Catal.* **1991**, *60*, 63.
(15) Clearfield, A. *Chem. Rev.* **1988**, *88*, 125.
(16) Fogg, A. M.; Dunn, J. S.; Shyu, S.-G.; Cary, D. R.; O'Hare, D. *Chem. Mater.* **1998**, *10*, 351.
(17) Davis, M. E.; Lobo, R. F. *Chem. Mater.* **1992**, *4*, 756.
(18) Haushalter, R. C.; Mundi, L. A. *Chem. Mater.* **1992**, *4*, 31.
(19) Soghomonian, V.; Haushalter, R.; Chen, Q.; Zubieta, J.; O'Connor, C. J.; Lee, Y.-S. *Chem. Mater.* **1993**, *5*, 1690.
(20) Soghomonian, V.; Chen, Q.; Haushalter, R.; Zubieta, J.; O'Connor, C. J. *Science* **1993**, *259*, 1596.
(21) Soghomonian, V.; Chen, Q.; Haushalter, R.; Zubieta, J. *Angew. Chem., Int. Ed. Engl.* **1993**, *32*, 610.
(22) Soghomonian, V.; Haushalter, R.; Chen, Q.; Zubieta, J. *Inorg. Chem.* **1994**, *33*, 1700.
(23) Khan, M. I.; Lee, Y.-S.; O'Connor, C. J.; Haushalter, R. C.; Zubieta, J. *Inorg. Chem.* **1994**, *33*, 3855.
(24) Zhang, Y.; Clearfield, A.; Haushalter, R. C. *J. Solid State Chem.* **1995**, *117*, 157.
(25) Zhang, Y.; Clearfield, A.; Haushalter, R. C. *Chem. Mater.* **1995**, *7*, 1221.
(26) Riou-Cavellec, M.; Serre, C.; Robino, J.; Noguès, M.; Grenèche, J.-M.; Férey, G. *J. Solid State Chem.* **1999**, *147*, 122.
(27) Korzenski, M. B.; Schimek, G. L.; Kolis, J. W. *J. Solid State Chem.* **1998**, *139*, 152.
(28) Korzenski, M. B.; Kolis, J. W. *J. Solid State Chem.* **1999**, *147*, 390.

10.1021/cm000356+ CCC: $19.00
Published on Web 09/15/2000

where subtle changes in a number of factors, including choice of template (if any), temperature, and pH, have substantial effects on the coordination environments of the metals and the dimensionality of the structures. Recently, O'Hare and co-workers reported the extension of organically templated hydrothermal syntheses of molecular, low-dimensional, and open-framework uranium-containing materials.[35−40] In particular, pH has been shown to be a determining factor in whether zero-, one-, two-, or three-dimensional structures form.[40] High-valent early transition metals, lanthanides, and actinides are logical choices for building structural flexibility in hydrothermal syntheses, as these metals show considerable variation in coordination number, geometry, and, in some cases, oxidation state.

Here we report the hydrothermal syntheses and structural characterization of two new organically templated U(IV) compounds, one-dimensional $(C_5H_{14}N_2)_2U_2F_{12}\cdot 2H_2O$ (**AU1-1**) and two-dimensional $(C_2H_{10}N_2)U_2F_{10}$ (**AU2-1**). The magnetic behavior of compounds containing U(IV) ions has generally been interpreted on the basis of a $5f^2$ configuration, which has a $^3H_4$ ground state.[41] However, complications arising from spin−orbit, crystal-field, and zero-field splitting effects on the temperature dependence of the susceptibility has led to a lack of detailed analysis of the magnetic behavior of low-dimensional uranium-containing compounds.[42] Previously, studies on monomeric octacoordinated U(IV) complexes have revealed effective moments ranging from 2.92 to 3.5 μ_B with Weiss constants Θ ranging from −50 to −200 K.[43] The effective moments for UCl_4 and UF_4 are 3.29 and 3.28 μ_B, respectively.[44] Neither of these compounds displays long-range magnetic ordering,[45] and specific heat measurements on UF_4 disclosed only a broad maximum attributed to a Schottky anomaly.[46] In compounds related to **AU2-1** containing $[U_2F_{10}]^{2-}$ layers, it has been shown that the U(IV) centers weakly interact antiferromagnetically through fluoride bridges.[35] We report below results which suggest magnetic interactions occurring within and between $[U_2F_{10}]^{2-}$ layers in **AU2-1** and describe the magnetism of the $[U_2F_{12}]^{2-}$ chains in **AU1-1**.

Experimental Section

Syntheses. UO_3 (99.8%, Alfa-Aesar), HF (48 wt %, Aldrich), and homopiperazine (98%, Aldrich) were used as received. Distilled and Millipore-filtered water was used in all reactions. The resistance of the water was 18.2 MΩ. *While the UO_3 contains depleted U, standard precautions for handling radioactive materials should be followed.* Elemental (CHN) microanalyses were performed by Atlantic Microlab, Inc. All reactions were run in Parr 4749 23 mL autoclaves with PTFE liners. The naming system for these compounds stands for Auburn University, the dimensionality of the structure, and the compound number.

$(C_5H_{14}N_2)_2U_2F_{12}\cdot 2H_2O$ (AU1-1) and $(C_2H_{10}N_2)U_2F_{10}$ (AU2-1). UO_3 (572 mg, 2 mmol) and homopiperazine (600 mg, 6 mmol) were loaded in a 23 mL PTFE-lined autoclave. Water (2 mL) was then added to the solids followed by the dropwise addition of HF (1.52 mL, 42 mmol). The autoclave was sealed and placed in a box furnace that had been preheated to 200 °C. After 72 h the furnace was cooled at 9 °C/h to 23 °C. The product consisted of a dark red-brown liquid over a mixture of large clusters of mint-green needles and isolated dark green crystals that can be approximated by truncated hexagonal bipyramids. The mother liquor was decanted from the crystals, which were then washed with methanol and allowed to dry; yield, 762 mg. Manual separation of these crystals showed each compound to be present in approximately equal quantities. The former crystals were subsequently identified as $(C_5H_{14}N_2)_2U_2F_{12}\cdot 2H_2O$, and the latter, as $(C_2H_{10}N_2)U_2F_{10}$. Anal. Calcd for $C_{10}H_{32}N_4F_{12}O_2U_2$: C, 12.72; H, 3.42; N, 5.93. Found: C, 11.88; H, 2.92; N, 5.44. Calcd for $C_2H_{10}N_2F_{10}U_2$: C, 3.30; H, 1.38; N, 3.85. Found: C, 3.47; H, 1.43; N, 3.86.

$(C_2H_{10}N_2)U_2F_{10}$ (AU2-1). UO_3 (286 mg, 1 mmol) and ethylenediamine (0.2 mL, 3 mmol) were loaded in a 23 mL PTFE-lined autoclave. Water (1 mL) was then added to the solids followed by the dropwise addition of HF (0.76 mL, 21 mmol). The autoclave was sealed and placed in a box furnace that had been preheated to 200 °C. After 72 h the furnace was cooled at 9 °C/h to 23 °C. The product consisted of an almost clear and colorless liquid over five isolated dark green crystals that had an approximately truncated hexagonal bipyramidal habit. Each of these crystals was larger than 0.3 cm on a side. The mother liquor was decanted from the crystals, which were then washed with methanol and allowed to dry; yield, 358 mg (98% yield). Anal. Calcd for $C_2H_{10}N_2F_{10}U_2$: C, 3.30; H, 1.38; N, 3.85. Found: C, 3.46; H, 1.43; N, 3.85.

Crystallographic Studies. Intensity data were collected from single crystals of **AU1-1** and **AU2-1** with the use of a Nicolet R3M diffractometer. Data collection for **AU1-1** was not straightforward because of twinning problems arising from the β angle being nearly 90° in the monoclinic unit cell. After 21 crystals were screened, all of which had β angles between 90.3 and 90.4°, only three were found to be well-behaved as ascertained by intensity scans. Data were collected in both $\omega/2\theta$ and pure ω scan modes on a crystal in which all 25 indexed reflections used to determine the unit cell were singular. Data for both compounds were processed, and analytical absorption corrections were applied. The structures were solved by direct methods and refined using the SHELXTL-93 package.[47] In these refinements, hydrogen atom positions were calculated with isotropic riding temperature factors. Some crystallographic details are listed in Table 1 for **AU1-1**

(29) Zima, V.; Lii, K.-H.; Nguyen, N.; Ducouret, A. *Chem. Mater.* **1998**, *10*, 1914.
(30) Riou-Cavellec, M.; Riou, D.; Férey, G. *Inorg. Chim. Acta* **1999**, *291*, 317.
(31) Feng, P.; Bu, X.; Stucky, G. D. *J. Solid State Chem.* **1997**, *129*, 328.
(32) Feng, P.; Bu, X.; Stucky, G. D. *J. Solid State Chem.* **1997**, *131*, 160.
(33) Feng, P.; Bu, X.; Tolbert, S. H.; Stucky, G. D. *J. Am. Chem. Soc.* **1997**, *119*, 2497.
(34) Mao, S.-Y.; Huang, Y.-X.; Wei, Z.-B.; Mi, J.-X.; Huang, Z.-L.; Zhao, J.-T. *J. Solid State Chem.* **2000**, *149*, 292.
(35) Francis, R. J.; Halasyamani, P. S.; O'Hare, D. *Chem. Mater.* **1998**, *10*, 3131.
(36) Francis, R. J.; Drewitt, M. J.; Halasyamani, P. S.; Ranganathachar, C.; O'Hare, D.; Clegg, W.; Teat, S. J. *Chem. Commun.* **1998**, 279.
(37) Francis, R. J.; Halasyamani, P. S.; O'Hare, D. *Angew. Chem., Int. Ed. Engl.* **1998**, *37*, 2214.
(38) Francis, R. J.; Halasyamani, P. S.; Bee, J. S.; O'Hare, D. *J. Am. Chem. Soc.* **1999**, *121*, 1609.
(39) Halasyamani, P. S.; Walker, S. M.; O'Hare, D. *J. Am. Chem. Soc.* **1999**, *121*, 7415.
(40) Walker, S. M.; Halasyamani, P. S.; Allen, S.; O'Hare, D. *J. Am. Chem. Soc.* **1999**, *121*, 10513.
(41) Hutchison, C. A., Jr.; Candela, G. A. *J. Chem. Phys.* **1957**, *27*, 707.
(42) (a) Fournier, J.-M.; Troæ, R. In *Handbook on the Physics and Chemistry of the Actinides*; Freeman, A. J., Lander, G. H., Eds.; Elsevier: New York, 1985; and references therein. (b) Martin, D. H. *Magnetism in Solids*; MIT Press: Cambridge, MA, 1967.
(43) Yoshimura, T.; Miyake, C.; Imoto, S. *Bull. Chem. Soc. Jpn.* **1974**, *47*, 515.
(44) Leask, M. J. M.; Osborne, D. W.; Wolf, W. P. *J. Chem. Phys.* **1961**, *34*, 2090.
(45) Erdos, P.; Robinson, J. M. *The Physics of Actinide Compounds*; Plenum Press: New York, 1983.
(46) Burns, J. H.; Osborne, D. W.; Westrum, E. F., Jr. *J. Chem. Phys.* **1960**, *33*, 387.
(47) Sheldrick, G. M. SHELXTL PC, Version 5.0, An Integrated System for Solving, Refining, and Displaying Crystal Structures from Diffraction Data; Siemens Analytical X-ray Instruments, Inc.: Madison, WI, 1994.

Table 1. Crystallographic Data for $(C_5H_{14}N_2)_2U_2F_{12}\cdot 2H_2O$ (AU1-1) and $(C_2H_{10}N_2)U_2F_{10}$ (AU2-1)

formula	$(C_5H_{14}N_2)_2U_2F_{12}\cdot 2H_2O$	$(C_2H_{10}N_2)U_2F_{10}$
formula mass (amu)	944.46	728.18
space group	$P2_1/c$ (No. 14)	$C2/c$ (No. 15)
a (Å)	9.272(4)	16.038(8)
b (Å)	12.314(4)	7.131(3)
c (Å)	18.475(7)	8.782(4)
b (deg)	90.32(3)	91.75(4)
V (Å3)	2109(1)	1003.9(8)
Z	4	4
T (°C)	22	22
λ (Å)	0.710 73	0.710 73
rcalcd (g cm3)	2.974	4.818
$\mu(M_o K_\alpha)$ (cm^{-1})	154.5	323.5
$R(F)$ for $F_o^2 > 2\sigma(F_o^2)$[a]	0.0618	0.0246
$R_w(F_o^2)$[b]	0.1220	0.0643

[a] $R(F) = \sum||F_o| - |F_c||/\sum|F_o|$. [b] $R_w(F_o^2) = [\sum[w(F_o^2 - F_c^2)^2]/\sum wF_o^4]^{1/2}$.

and **AU2-1**. Additional crystallographic details are given in the Supporting Information.

Magnetic Measurements. Magnetic data were measured on powders in gelcap sample holders with a Quantum Design PPMS 9T magnetometer/susceptometer between 2 and 300 K and in applied fields up to 9 T. AC susceptibility measurements were made with a driving amplitude of 1 Oe and frequencies between 10 and 2000 Hz. DC susceptibility measurements were made under zero-field-cooled conditions with an applied field of 0.5 T. Susceptibility values were corrected for the sample diamagnetic contribution according to Pascal's constants[48] (**AU1-1**, -98×10^{-6} emu/f.u.; **AU2-1**, -232×10^{-6} emu/f.u.) as well as for the sample holder diamagnetism.

Results and Discussion

Syntheses. The reaction of UO_3 with HF and homopiperazine ($C_5H_{12}N_2$) at 200 °C in aqueous media for 72 h results in the formation of $(C_5H_{14}N_2)_2U_2F_{12}\cdot 2H_2O$ (**AU1-1**) and $(C_2H_{10}N_2)U_2F_{10}$ (**AU2-1**) in an approximately equal molar ratio. While this reaction is obviously complex, several conclusions can be drawn. First, reduction of U(VI) to U(IV) occurs, with concomitant oxidation of water most likely taking place. However, as the homopiperazine is in excess, its oxidation cannot be ruled out. Second, ring cleavage of the homopiperazine occurs to produce diprotonated ethylenediamine and 1,3-difluoropropane. Third, whereas the latter simply leaves as a gas, the former serves to template the formation of **AU2-1**. The ring cleavage is driven by the elevated temperatures and the presence of the HF, which serves as a source of both protons and nucleophilic F^- ions. The extra ring strain in homopiperazine certainly enhances ring cleavage, as such reactions were not reported in the piperazine and 2-methyl-piperazine uranium fluoride and oxyfluoride systems.[37−40] Reactions were run at lower temperatures (160 and 180 °C) and with decreased amounts of HF in an effort to prepare **AU1-1** in pure form. These reactions, however, resulted in a different series of compounds that will be reported separately.[49] Product composition was not significantly affected by reducing the reaction duration to 48 h.

Despite the mixture of products resulting from this reaction, pure samples can be easily obtained through manual separation of the crystals. $(C_5H_{14}N_2)_2U_2F_{12}\cdot 2H_2O$ forms large clusters of mint-green needles that are often large enough to isolate with tweezers. In contrast, $(C_2H_{10}N_2)U_2F_{10}$ forms large, well-formed, dark green crystals with an approximately hexagonal bipyramidal habit. We observed that by increasing the reaction duration to 5 days, considerably larger crystals could be grown, which facilitates product separation.

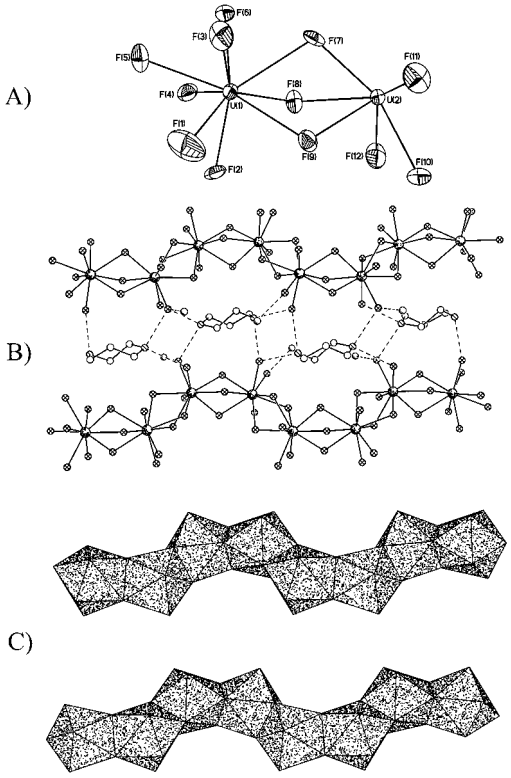

Figure 1. AU1-1: (a) asymmetric unit for a $[U_2F_{12}]^{4-}$ chain (here and in Figure 2a, 50% displacement ellipsoids shown); (b) part of the hydrogen-bonding network in $(C_5H_{14}N_2)_2U_2F_{12}\cdot 2H_2O$; (c) polyhedral representation of the $[U_2F_{12}]^{4-}$ chains showing face-sharing tricapped trigonal prisms.

The direct reaction of UO_3 with HF and ethylenediamine at 200 °C for 72 h produces $(C_2H_{10}N_2)U_2F_{10}$ in 98% yield. In this particular reaction the crystals produced exceed 0.3 cm on average per edge with one crystal measuring 0.7 cm. This result is somewhat surprising as O'Hare and co-workers found that closely related uranium fluorides with $^+H_3N(CH_2)_nNH_3^+$ (n = 3, 4, 6) templates could only be prepared when phosphoric acid was added to the reaction mixtures.[35] The difference between our reactions and those of O'Hare and co-workers may stem from our source of uranium (UO_3 instead of UO_2) or from our increased reaction time (72 h instead of 24 h).[35]

Structures. $(C_5H_{14}N_2)_2U_2F_{12}\cdot 2H_2O$ (AU1-1). AU1-1 is composed of one-dimensional chains of $[U_2F_{12}]^{4-}$ extended along [010] that are separated by homopiperazine dications and water molecules, all of which form a hydrogen-bonding network.[38] This structure is only the second example of a one-dimensional uranium fluoride compound. The asymmetric unit for the $[U_2F_{12}]^{4-}$ anion is shown in Figure 1a, and part of the hydrogen-bonding network is depicted in Figure 1b. Selected bond distances are given in Table 2. The water molecules reside in small channels approximately 6.7 Å across that

(48) Mulay, L. N.; Boudreaux, E. A. *Theory and Applications of Molecular Diamagnetism*; Wiley-Interscience: New York, 1976.

(49) Almond, P. M.; Deakin, L.; Porter, M. J.; Mar, A.; Albrecht-Schmitt, T. E. *Inorg. Chem.*, manuscript in preparation.

Table 2. Selected Bond Distances (Å) for $(C_5H_{14}N_2)_2U_2F_{12}\cdot 2H_2O$ (AU1-1) and $(C_2H_{10}N_2)U_2F_{10}$ (AU2-1)

	$(C_5H_{14}N_2)_2U_2F_{12}\cdot 2H_2O$		
U(1)−F(1)	2.277(13)	U(2)−F(4)	2.386(11)
U(1)−F(2)	2.249(11)	U(2)−F(5)	2.390(11)
U(1)−F(3)	2.210(11)	U(2)−F(6)	2.371(10)
U(1)−F(4)	2.435(11)	U(2)−F(7)	2.291(11)
U(1)−F(5)	2.372(11)	U(2)−F(8)	2.410(10)
U(1)−F(6)	2.368(10)	U(2)−F(9)	2.381(11)
U(1)−F(7)	2.465(10)	U(2)−F(10)	2.313(11)
U(1)−F(8)	2.295(11)	U(2)−F(11)	2.221(11)
U(1)−F(9)	2.357(11)	U(2)−F(12)	2.203(11)
U(1)−U(2)	3.739(2)	U(1)−U(2)′	3.744(1)
	$(C_2H_{10}N_2)U_2F_{10}$		
U(1)−F(1)	2.307(5)	U(1)−F(1)′	2.331(5)
U(1)−F(2)	2.324(5)	U(1)−F(2)′	2.367(5)
U(1)−F(3)	2.214(6)	U(1)−F(4)′	2.459(5)
U(1)−F(4)	2.325(5)	U(1)−F(5)′	2.322(5)
U(1)−F(5)	2.371(6)	U(1)−U(1)′	3.9476(14)
		U(1)−U(1)″	3.8884(14)

extend down [100] and [010]. The $[U_2F_{12}]^{4-}$ chains are formed from face-sharing interactions between nine-coordinate UF_9 polyhedra that can be roughly described as tricapped trigonal prisms. A polyhedral representation of this chain is depicted in Figure 1c. As each polyhedron has two such face-sharing arrangements, the coordination environment around each U(IV) center can be described as $[UF_{6/2}F_{3/1}]^{4-}$. The U−F bridging and terminal distances range from 2.295(11) to 2.465(10) and 2.203(11) to 2.313(11) Å, respectively. Two independent U−U distances of 3.739(2) and 3.744(1) Å are found. The bond valence sums for U(1) and U(2) are 4.09 and 4.14, respectively. These results are consistent with the assignment of U(IV) and indicate that the substitution of oxide for fluoride in **AU1-1** is unlikely. This structure differs from the related molecular $(C_5H_{14}N_2)_2(H_3O)U_2F_{13}$ (**UFO-5**) and one-dimensional $(C_5H_{14}N_2)_2U_2F_{13}\cdot H_2O$ (**UFO-6**) structures in several respects.[38] While the $[U_2F_{13}]^{5-}$ dimers in **UFO-5** are also formed by face-sharing through three bridging fluoride ligands, each U(IV) center is only eight-coordinate. Like **AU1-1**, the structure of **UFO-6** also contains one-dimensional $[U_2F_{12}]^{4-}$ chains, but each U(IV) center is only eight-coordinate and the UF_8 polyhedra are joined only through edge-sharing.

$(C_2H_{10}N_2)_2U_2F_{10}$ (AU2-1). AU2-1 is a layered compound with $[U_2F_{10}]^{2-}$ layers separated by diprotonated ethylenediamine. Each layer consists of UF_9 tricapped trigonal prisms (Figure 2a) that share two edges and three corners with neighboring polyhedra. F(3) is not involved in bonding within each layer and points between layers. Selected bond distances are given in Table 2. A view along [010] shows the layered structure with the cations separating the layers (Figure 2b). A polyhedral representation of a $[U_2F_{10}]^{2-}$ layer viewed down the *a* axis showing edge- and corner-sharing UF_9 tricapped trigonal prisms is depicted in Figure 2c. **AU2-1** represents the $n = 2$ member of the series of compounds $(H_3N(CH_2)_nNH_3)U_2F_{10}$ previously found for **UFO-1** ($n = 3$), **UFO-2** ($n = 5$), and **UFO-3** ($n = 6$).[35] In **AU2-1**, the diamines lie at 34.8° relative to the uranium fluoride planes, which is substantially more acute than the diamines in **UFO-1**, **UFO-2**, or **UFO-3**, which lie at 90, 85, and 75°, respectively.[35] This results in a shorter than expected interlayer spacing of 8.0 Å, compared to distances of 10.7, 11.5, and 13.1 Å for **UFO-1**, **UFO-2**, and **UFO-3**, respectively.[35]

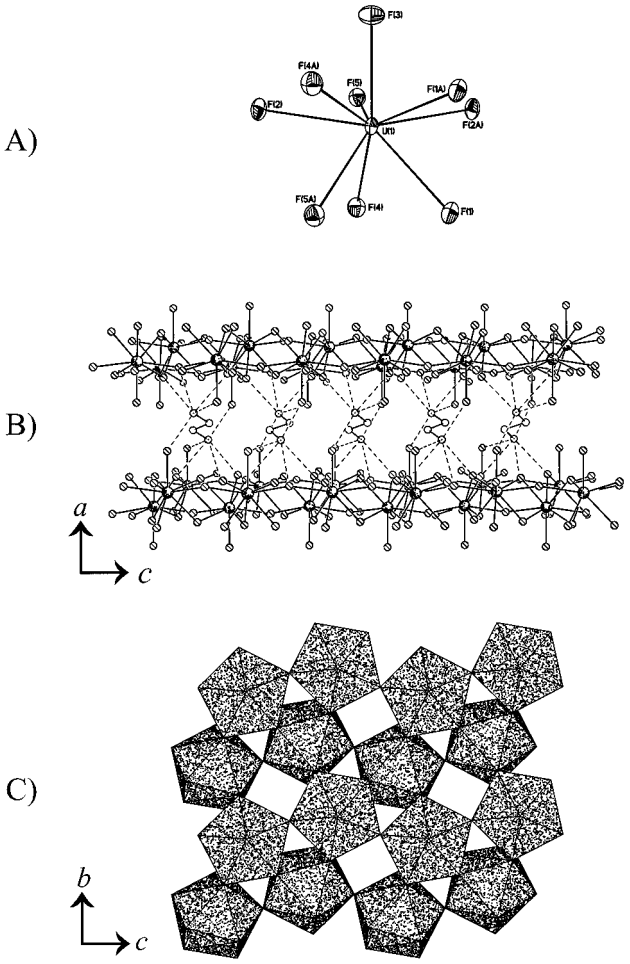

Figure 2. AU2-1: (a) UF_9 tricapped trigonal prisms in the layers of $(C_2H_{10}N_2)U_2F_{10}$; (b) view along [010] shows the layered structure with ethylenediamine dications separating the layers; (c) polyhedral representation of a $[U_2F_{10}]^{2-}$ layer viewed down the *a* axis showing edge- and corner-sharing UF_9 tricapped trigonal prisms.

Magnetic Properties. The effective moment at 300 K for **AU1-1** is 4.37 μ_B/f.u. (3.09 μ_B/U(IV)). This value is lower than the value of 3.58 μ_B/U(IV) expected according to Russell−Saunders coupling ($g_J = 4/5$ and $J = 4$) for a $^3H_4$ ground state. A fit of the magnetic susceptibility above 150 K results in $\Theta = -1.3$ K. The effective moment decreases rapidly below ~50 K with decreasing temperature (Figure 3a), suggesting the presence of antiferromagnetic interactions, although the presence of zero-field splitting for this $5f^2$ ion and a nonmagnetic ground state may also be contributing to this change in moment. Our analysis assumes that no dehydration of **AU1-1** occurs during the magnetic measurement. Since their contribution to the formula weight is small, even allowing for the loss of the two water molecules would only result in a negligible change in the moment to μ_{eff}(300 K) = 4.28 μ_B/f.u.

The field dependence of the magnetization of **AU1-1** at 2 K (Figure 4a) displays a change in slope at H_c = 3.60 T, similar to that observed for metamagnetic transitions.[50] The nonlinear nature of the magnetization and the unusual transition observed is not consistent

(50) DeJongh, L. J.; Miedema, A. R. *Experiments on Simple Magnetic Model Systems*; Taylor & Francis: London, 1974.

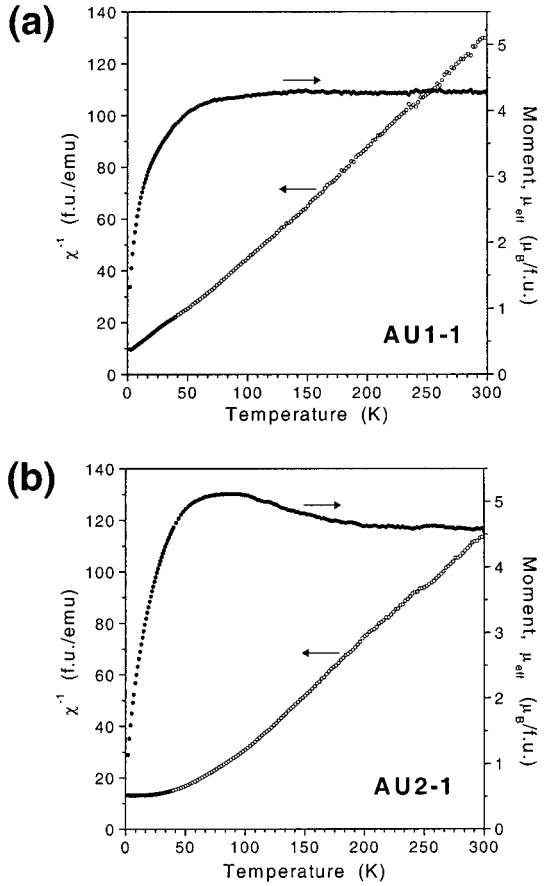

Figure 3. Temperature dependence of the effective moment (filled symbols) and reciprocal molar magnetic susceptibility (open symbols) for (a) **AU1-1** and (b) **AU2-1** under an applied magnetic field of 0.5 T.

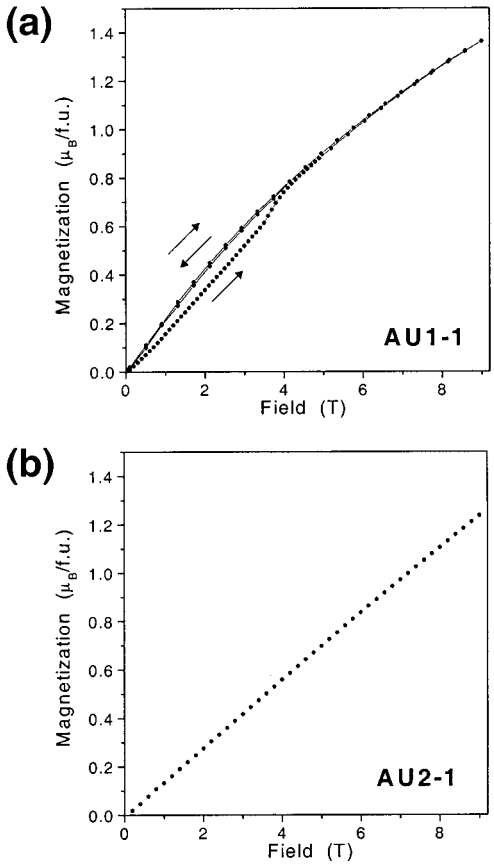

Figure 4. Field dependence of magnetization at 2 K for (a) **AU1-1** (lines are included to guide the eye) and (b) **AU2-1**.

with the presence of a U(IV) nonmagnetic ground state and suggests the presence of nonnegligible 1-D magnetic interactions. Cycling the field from 9 T → −9 T → 9 T then leads to an anhysteretic magnetization loop (M_{9T} = 0.68 μ_B/U(IV)). The field-induced transition is irreversible as the magnetization does not retrace the transition at H_c. **AU1-1** does not display a maximum in χ' (in-phase linear) magnetic susceptibility, which is characteristic of materials undergoing long-range antiferromagnetic ordering, placing T_N < 2 K. Therefore, the irreversible metamagnetic-like transition observed in the isothermal magnetization at 2 K cannot be clearly assigned. The possible contribution from paramagnetic impurities to the susceptibility may be significant at very low temperatures, masking a maximum in χ'. Detailed magnetic characterizations of other low-dimensional uranium(IV) compounds are then required to develop a deeper understanding of the magneto−structural relationships present in these types of materials.

The effective moment at 300 K for **AU2-1** is 4.58 μ_B/f.u. (3.23 μ_B/U(IV)). Although this value is similar to that for UF_4 (3.28 μ_B/U(IV)),[44] it is somewhat lower than those reported for other members $(H_3N(CH_2)_nNH_3)U_2F_{10}$ with greater n (4.91−5.66 μ_B/f.u.).[35] The increase in effective moment with decreasing temperature, which is reproducible, is clearly observed (Figure 3b) and results in a positive paramagnetic Curie−Weiss temperature of Θ = +21 K (150 < T < 300 K). This Θ value is very different from that for the other $(H_3N(CH_2)_n$-$NH_3)U_2F_{10}$ compounds (Θ = −25 to −42 K).[35] The observation of a spontaneous moment, manifested here as a broad maximum in the temperature dependence of the effective moment, is likely a result of spin canting. This is attributed to the presence of short-range weak ferromagnetic interactions within the $[U_2F_{10}]^{2-}$ layers in **AU2-1**. The effective moment then decreases sharply with further decreasing temperature. Although this may result from antiferromagnetic interactions between the layers, the tendency of the susceptibility to a temperature-independent value of 0.076 emu/f.u. below 15 K may also indicate that the ground state of the U(IV) ions is nonmagnetic.[45] The magnetization for **AU2-1** at 2 K (Figure 4b) is essentially linear with field up to 9 T (M_{9T} = 1.24 μ_B/f.u.) and does not display field-dependent behavior similar to **AU1-1**. Low-temperature AC magnetic susceptibility measurements do not display a maximum but show a rapid increase in χ' below 4 K, which could arise from small amounts of paramagnetic impurities. It is conceivable that the magnetic behavior of **AU2-1** is a result of a complex electronic ground state of the compound, similar to UF_4 in which two-thirds of the U(IV) ions have a nonmagnetic singlet ground state.[44]

Acknowledgment. This work was supported by NASA (Alabama Space Grant Consortium), NASA-EPSCoR, and Auburn University in the form of start-up funds, a competitive research grant, and a Dean's Research Initiative Grant. Financial support from the NSERC (Canada) and the University of Alberta is gratefully acknowledged.

Supporting Information Available: Tables giving structure determinations summaries, positional coordinates, and equivalent isotropic displacement parameters, bond lengths and angles, and anisotropic displacement parameters for **AU1-1** and **AU2-1**. This material is available free of charge via the Internet at http://pubs.acs.org.

CM000356+